

Photosensitivity of optical fibres doped with different impurities

Yu.V. Larionov, A.A. Rybaltovsky, S.L. Semenov, S.K. Vartapetov, M.A. Kurzanov, A.Z. Obidin

Abstract. Photosensitivities of hydrogen-loaded silica fibres doped with germanium, phosphorus, antimony, and aluminium are estimated and compared. It is shown that although all the fibres can be pre-exposed, the degree of this effect is noticeably different for different fibres because the induction of the refractive index is determined by a combined contribution from a one-step photochemical reaction and a two-step reaction responsible for pre-exposure. One-step reactions dominate in more photosensitive optical fibres, while two-step reactions dominate in less photosensitive fibres.

Keywords: photosensitivity, pre-exposure, glass defects, induced refractive index, excimer laser.

1. Introduction

The possibility of changing the refractive index in silica optical fibres exposed to UV radiation was discovered long ago and is now widely used, for example, for manufacturing sensors and telecommunication devices based on fibre Bragg gratings (FBGs) produced in the refractive index of an optical fibre. However, many details of the mechanism of a variation in the refractive index still remain unknown. Moreover, some new manifestations of variations in the refractive index were found quite recently, in particular, the pre-exposure effect [1].

The photosensitivity of optical fibres (the capability to change their refractive index upon exposure to UV radiation) in the initial state is, as a rule, low for practical applications; however, it noticeably increases when fibres are loaded with molecular hydrogen. It was found in Ref. [1] that a fibre can be sensitised, resulting in a noticeable increase in its photosensitivity in the absence of H₂ molecules inside the fibre. The sensitising is performed by exposing a hydrogen-loaded fibre to a homogeneous UV beam using a comparatively low exposure dose (compared to the dose required to write the FBG). This

procedure is called pre-exposure. Once H₂ molecules have left the fibre, the latter can have an enhanced photosensitivity for a long time. The fibre sensitising achieved due to pre-exposure was first discovered for germanosilicate fibres (GSFs) [1], then for phosphosilicate fibres (PSFs) [2], and recently for alumina- and antimony-silicate fibres [3, 4]. It seems that this effect is inherent in silica fibres.

The fibre sensitisation caused by pre-exposure was explained in Ref. [5], where it was assumed that this effect appears due to a two-step photochemical reaction modifying point defects in the fibre core. At the first stage of this reaction, two hydrogen atoms are formed from a hydrogen molecule, which fit into the initial defects of the glass. The initial defects modified this way become intermediate defects. They do not change the refractive index directly, but can be modified by UV radiation even in the absence of molecular hydrogen to the final defects, which cause the induction of the refractive index at the second stage of the photochemical reaction.

By now several mechanisms were proposed to explain the induction of the refractive index in silica fibres caused by UV irradiation. All these mechanisms (and their combination) assume that variations in the refractive index are induced during one stage of photochemical transformations of the initial states or structures to the final ones (see, for example, Ref. [6]). The existence of two-step photochemical reactions in fibres poses the question about the relation between one-step and two-step reactions, in particular, whether the two-step process of the induction of the refractive index is the only one, predominant, or accompanies the one-step process. This problem was investigated in Ref. [7], however, the answer was obtained only for PSFs.

The aim of this paper is to find the presence of two-step and one-step photochemical processes in silica fibres doped with different impurities and to estimate the relation between them.

2. Experimental

We studied optical fibres doped with four different chemical elements, for which the pre-exposure effect has been already observed experimentally. They included GSFs, PSFs, and also fibres doped with antimony and aluminium. Fibres doped with germanium and phosphorus, whose photosensitivity had been studied most thoroughly, were investigated in our experiments at different impurity concentrations. The molar content of phosphorus oxide in PSFs with low optical losses [8] was 10.2% ($\Delta N = 0.009$, $\lambda_c = 1.03 \mu\text{m}$) and 12.5% ($\Delta N = 0.01$, $\lambda_c = 1.1 \mu\text{m}$).

Yu.V. Larionov, A.A. Rybaltovsky, S.L. Semenov Fiber Optics Research Center, A.M. Prokhorov General Physics Institute, Russian Academy of Sciences, ul. Vavilova 38, 119991 Moscow, Russia;
S.K. Vartapetov, M.A. Kurzanov, A.Z. Obidin Physics Instrumentation Center, A.M. Prokhorov General Physics Institute, Russian Academy of Sciences, 142190 Troitsk, Moscow region, Russia

Received 4 August 2003

Kvantovaya Elektronika 34 (2) 175–179 (2004)

Translated by M.N. Sapozhnikov

Below, we will refer to these fibres as P10.2 and P12.5, respectively. The molar content of germanium in GSFs was 3.5% (an analogue of the Corning SMF 28, $\Delta N = 0.005$, $\lambda_c = 1.24 \mu\text{m}$, denoted by SM28) and 4.5% (an analogue of the Flexcore, $\Delta N = 0.0065$, $\lambda_c = 0.96 \mu\text{m}$, denoted by Flxc). The molar concentration of antimony oxide in a Sb-doped fibre was 1% ($\Delta N = 0.01$, $\lambda_c = 1.03 \mu\text{m}$). In fibres doped with aluminium and erbium, the molar content of Al_2O_3 was 9% and the mass content of Er^{3+} was 0.6% ($\Delta N = 0.0206$, $\lambda_c = 0.98 \mu\text{m}$). The concentration of oxides was measured at the fibre cross section with an X-ray microanalyser of a JSM-5910LV (JEOL) electron microscope.

The necessity to compare fibres that can have different photosensitivities imposes strict requirements to the method of measuring the induced refractive index and to the reproducibility of experimental conditions upon the preparation of fibres for exposure and during the exposure itself.

The refractive index induced in fibres is measured, as a rule, by the FBG writing method. At the preliminary stage of our study, we measured the photosensitivity of fibres by the FBG writing method and by the interferometric method. Principles and details of these experiments are described in Ref. [7]. The results of measurements of the induced refractive index by these two methods are noticeably different. The data obtained by the interferometric method revealed some features of the photosensitivity of different fibres, which were not found by the FBG writing method. In addition, the reproducibility of the values of the induced refractive index obtained by the interferometric method is better than that in the FBG method. This is explained by the following metrological disadvantages of the latter method compared to the interferometric method:

(i) The difficulty of detecting the instant of appearance of a peak reflected from the FBG at low exposure doses and the limited ability of measuring the amplitude of this peak at high exposure doses, which is determined by the technical parameters of a spectrum analyser. This narrows down the range of exposure doses within which the photosensitivity of fibres can be measured.

(ii) The dynamics of FBG writing strongly depends on the degree of coherence of excimer-laser radiation. It is different for different lasers and depends on the laser adjustment and the FBG writing scheme. The dependence of the induced refractive index on the coherence of light used for FBG writing impairs its reproducibility and impedes a comparison of its values obtained with the help of different excimer lasers.

(iii) The reproducibility of the induced refractive index in the FBG method depends on the gap between the fibre and the phase mask used to produce the FBG. The induced refractive index was not reproduced in our experiments because we could not control the gap value in this method.

(iv) Light incident on the phase mask is distributed not only into the 1st and -1 st diffraction orders but also into other diffraction orders. This reduces the contrast of the interference pattern being formed, resulting in the distortion of the distribution of the induced refractive index at high exposure doses.

For this reason, we prefer the interferometric method, and will below present the estimates of the induced refractive index performed by this method only.

The reproducibility of conditions for inducing the refractive index in the fibres was provided in the following way. All the fibres under study were equally loaded with

molecular hydrogen at an external pressure of 100 atm and temperature 100°C . They were irradiated by CL-5000, CL-7000 [9], and Lumonics-520 (Lum) excimer lasers at a wavelength of 193 nm with the same pulse energy density for results being compared. The laser pulse repetition rate was 10 Hz in all experiments.

3. Results and discussion

Figure 1 shows the results of measurements of the induced refractive index in different fibres. The characteristic feature of the curves in Fig. 1 is a great scatter in the exposure doses at which the induced refractive index at the level of $10^{-5} - 10^{-4}$ is achieved and a small scatter in the doses for the induction of the refractive index at the level of $10^{-3} - 5 \times 10^{-3}$, i.e., the curves are drawing together with increasing the exposure dose.

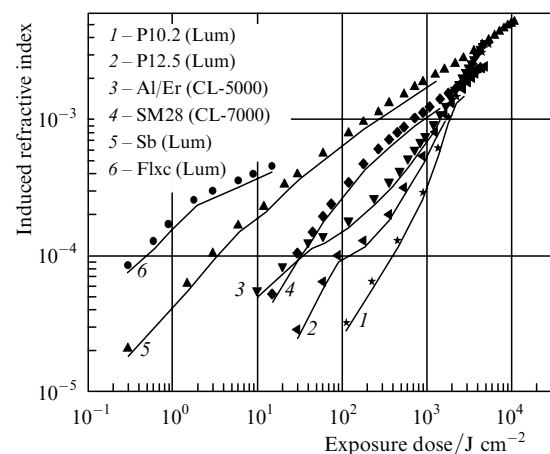


Figure 1. Dose dependences of the induced refractive index of H_2 -loaded fibres. The pulse energy density for curves (1), (2), (3), (5), and (6) is 300 mJ cm^{-2} and 200 mJ cm^{-2} for curve (4). The fibre types and lasers are indicated for each curve.

Another feature of these curves is a different type of the increase in the refractive index for different fibres. Curves (4, 5, 6) at the left in Fig. 1 demonstrate the increase in the refractive index in fibres having a relatively high photosensitivity in the range of low exposure doses. They increase almost linearly in this range at a double logarithmic scale and tend to saturate at high doses. Curves (1, 2, 3) at the right in Fig. 1 obtained for fibres with a lower photosensitivity increase differently. They have the region of a linear increase at low doses [up to 100 J cm^{-2} for curve (2); this region being virtually absent in curve (1)], which is followed by the region of a slow increase. Then, a faster increase is observed and, finally, the increase slows down and the dependence is saturated. This type of the dependence is called S-like in the literature [10].

A gradual change in the shape of curves (6–1) from the first type of behaviour to the second one suggests that there exists a property of the photosensitivity, which is inherent in all the fibres and is manifested differently in fibres with high and low photosensitivity, being intermediate for fibres with a moderate photosensitivity. We assumed that this property is related to the pre-exposure effect. To verify this assumption, we estimated the photosensitivity of the fibres for three exposure regimes: for hydrogen-loaded fibres, after pre-

exposure, and in the initial state, i.e., in the absence of hydrogen-loading (Table 1). The values of the induced refractive index were measured for the exposure dose equal to 1 kJ cm^{-2} . The pre-exposure dose for PSFs and GSFs was selected to achieve the maximum value of the induced refractive index during exposure at the second stage (~ 2 [11] and $\sim 0.1 \text{ kJ cm}^{-2}$ [5], respectively). For antimony- and aluminium-doped fibres, the pre-exposure doses were 1 and 1.2 kJ cm^{-2} , respectively.

Table 1.

Dopant	Molar concentration (%)	ΔN_{ind}		
		H ₂ -loaded fibre	Pre-exposed fibre	Initial fibre
Sb ₂ O ₃	1	1.5×10^{-3}	7×10^{-4}	6×10^{-4}
GeO ₂	3.5	1.5×10^{-3}	6×10^{-4}	4×10^{-4}
Al ₂ O ₃ /Er	9	7×10^{-4}	5×10^{-4}	8.5×10^{-5}
P ₂ O ₃	12	4×10^{-4}	6×10^{-4}	3×10^{-5}

The pre-exposure effect in different fibres can be estimated from the value of induced refractive index in a pre-exposed fibre compared to the induced refractive index in the initial and hydrogen-loaded fibres. The pre-exposure effect is manifested most noticeably in PSFs. One can see from Table 1 that the induced refractive index in the pre-exposed PSF even exceeds that in the hydrogen-loaded fibre (6×10^{-4} and 4×10^{-4} , respectively). The pre-exposure effect is the weakest in antimony-doped fibres. In this case, the induced refractive index in the pre-exposed fibre only slightly exceeded that in the initial fibre. The pre-exposure effect in the GSF was stronger than in the antimony-silicate fibre but weaker than in alumina-silicate fibre. Therefore, the strength of pre-exposure effect correlates with the position of curves in Fig. 1 (decreases from the left to right).

It was shown in Ref. [7] that the S-like dose dependence is related to a two-step photochemical reaction proceeding in the fibre. The S-like dependence is typical for fibres doped with phosphorus [curves (1) and (2) in Fig. 1]. This dependence was also observed for aluminium-doped fibres [curve (3)]. The absence of the S-like shape for curves (4–6) in Fig. 1 suggests that the influence of two-step photochemical reactions on the induced refractive index in these fibres is limited.

The shape of curves (4–6) in Fig. 1 can be explained assuming that the refractive index is induced in different hydrogen-loaded fibres due to two simultaneous photochemical reactions. The first, one-step reaction modifies the initial defects directly to the final defects, which change the refractive index. The second reaction occurs in two steps. The relative intensities of these photochemical reactions in different fibres are probably noticeably different. In our opinion, the one-step reaction dominates in fibres with the photosensitivity depicted by curves (4–6). The induced refractive index described by curves (1–3) is determined by the increasing influence of the two-step reaction.

The first evidence about the proceeding of one-step and two-step photochemical reactions in one fibre was obtained in Ref. [7] for the PSF based on the analysis of the derivative of the dose dependence of the induced refractive index over the dose $d(\Delta N_{\text{ind}})/dD$. It was found that changes in the derivative reflect the dynamics of the concentration of defects of different types preceding the formation of final

defects. It was also found that the concentration of intermediate defects in the PSF increases rather slowly (compared to GSFs [5]) and achieves a maximum for the dose of $\sim 2000 \text{ J cm}^{-2}$. The concentration of defects of other type involved only in the one-step reaction occurs in the dose range between 0 and 500 J cm^{-2} . These variations in the concentration of defects of different types occur in different ranges of the exposure dose, and can be therefore detected independently. We can assume that one-step and two-step reactions occur in other fibres studied in this paper [curves (4–6) in Fig. 1] in the same range of the exposure dose. In this case, a more active one-step photochemical reaction can mask the manifestation of a less active two-step reaction.

By describing the dynamics of the defect concentration using the same basic mathematical expressions as in Ref. [7], we obtain the equations for simultaneous variations in the concentration of defects involved in one-step and two-step photochemical reactions. We assume for simplicity that the same initial defects give rise to the intermediate defects in the two-step photochemical reaction and to the final defects in the one-step reaction. Then, using the model proposed in Ref. [5], the equations can be written in the form

$$\begin{aligned}
 \dot{A} &= -(v_1^\dagger + v^\circ)A, \\
 \dot{B} &= v_1^\dagger A - v_2^\dagger B, \\
 \dot{C}^\dagger &= v_2^\dagger B, \\
 \dot{C}^\circ &= v^\circ A,
 \end{aligned} \tag{1}$$

where A is the concentration of initial defects, which are transformed in the two-step reaction to intermediate defects with the concentration B and in the one-step reaction to the final defects with the concentration C° . C^\dagger is the concentration of defects produced after the destruction of intermediate defects at the second stage in the two-step reaction. The concentration of initial defects changes at the rate v_1^\dagger during the formation of intermediate defects in the two-step reaction and at the rate v° during the formation of final defects in the one-step reaction. The rate v_2^\dagger determines the rate of transformation of intermediate defects to final defects at the second stage of the two-step photochemical reaction.

We assume that a change in the induced refractive index is proportional to the concentration $C^\circ + C^\dagger$ of final defects. Then, it follows from (1) that, by measuring a change in the induced refractive index, we can determine the dynamics of variation in the quantity $A^\circ + B$, where A° is a part of initial defects A that is involved only in the one-step photochemical reaction. Indeed, the derivative dC^\dagger/dD of the concentration of final defects is proportional to the concentration B of intermediate defects, while dC°/dD is proportional to A° and the sum of these derivatives is proportional to $A^\circ + B$.

Figure 2 shows the dose dependences of the concentration A^\dagger of initial defects in the two-step reaction [curve (1)] and the concentration A° of initial defects in the one-step reaction [curve (2)], as well as the dose dependence of the concentration B of intermediate defects [curve (3)] and the sum $A^\circ + B$ for the case when $v_1^\dagger = v_2^\dagger$ and $v^\circ = 0.25v_1^\dagger$ [curve (4)] and when $v^\circ = 0.13v_1^\dagger$ [curve (5)]. The total concentration $A^\circ + B$ is a stepwise decreasing function.

However, the stepwise decrease of the function is almost unnoticeable when the rate of the one-step reaction exceeds that of the two-step reaction. When the activity of the one-step reaction decreases compared to that of the two-step reaction, the stepwise character of the dependence increases and later a minimum appears [curve (5)]. All these variations are observed in the dose range where the concentration B of intermediate defects increases and achieves its maximum.

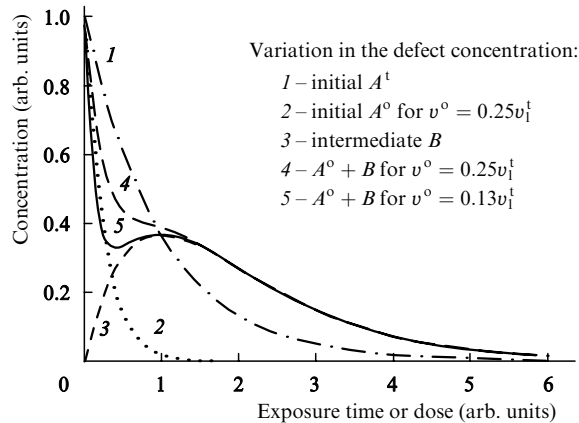


Figure 2. Normalised dose dependences of the concentration of defects calculated from (1).

The correctness of theoretical predictions about the stepwise dose dependence of the defect concentration in the case of simultaneous one-step and two-step reactions can be verified experimentally using the data presented in Fig. 1.

Figure 3 shows the derivatives of the dose dependences of the induced refractive index taken from Fig. 1. They reflect the dynamics of the concentration of defects preceding the formation of final defects. The stepwise change in the defect concentration $A^o + B$ can be found in curves (3–5) in Fig. 3 in the dose range from 10 to 10^3 J cm^{-2} , and the minimum is observed for curve (2). It is interesting that the stepwise change in the defect concentration for curves (4)

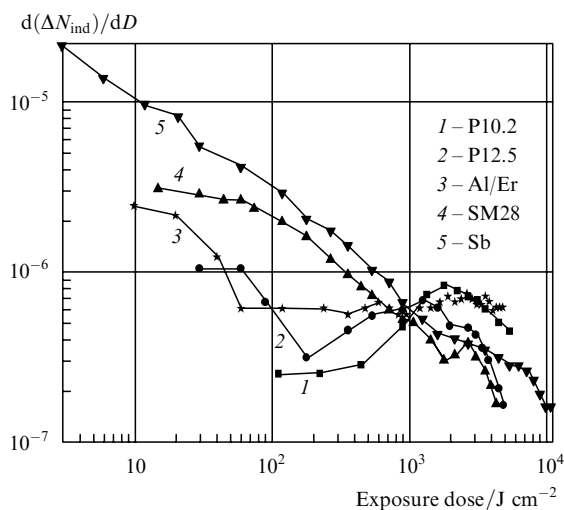


Figure 3. Dose dependences $d(\Delta N_{\text{ind}})/dD$ for the induced refractive-index curves presented in Fig. 1

and (5) is again observed in the range $10^3 - 10^4$ J cm^{-2} [i.e., beyond the range of a high photosensitivity of fibres doped with germanium and antimony (see Fig. 1)]

The highest concentration $A^o + B$ of defects at the beginning of the exposure was observed for most photosensitive fibres doped with antimony, this concentration was lower in fibres doped with germanium, still lower in aluminium-doped fibres, and the lowest concentration was observed in fibres doped with phosphorus at the molar concentration of 12.5% (Fig. 3). The initial defects of the A^o type were not virtually observed in fibres doped with $\sim 10\%$ of phosphorus oxide. This suggests that the activity of the one-step reaction with respect to the two-step reaction is maximal for curve (5) and gradually decreases for curves (4–1). In our opinion, this effect is also manifested in the shape and width of steps in the curves in Fig. 3. A barely noticeable step in curves (5) and (4) becomes wide in curve (3), and then a dip appears in the step in curve (2) [cf. with curves (4) and (5) in Fig. 2]. All this means that the photosensitivity of optical fibres in the exposure range from 10 to 10^3 J cm^{-2} is mainly determined by one-step photochemical reactions.

One can see from Fig. 3 that for exposure doses exceeding 1 kJ cm^{-2} , the dose dependence of the concentration for both PSFs [curves (1) and (2)] has a maximum in the range $1.3 - 1.8$ kJ cm^{-2} . It was shown in Ref. [7] that these maxima reflect the dynamics of variation in the concentration B of intermediate defects. The greater value of B is achieved in the fibre with a lower concentration of phosphorus [cf. curves (1) and (2)]. This means formally that the two-step reaction occurs more actively at a lower concentration of phosphorus.

We cannot explain the presence of the step in the dose dependence of the induced refractive index at doses above 1 kJ cm^{-2} for the antimony-doped fibre [curve (5)] and the existence of the maximum and minimum for the germanium-doped fibre [curve (4)]. Probably they are related to other two-step reactions proceeding in these fibres.

Thus, the shape of all curves in Fig. 3 (and, hence, in Fig. 1) at the exposure doses below 1 kJ cm^{-2} can be explained by the combined action of one-step and two-step photochemical reactions. One can see from Fig. 3 that, when the one-step photochemical reaction dominates [curves (4–6) in Fig. 1], the two-step reaction is weakly manifested. The situation is opposite for curve 1. Only in the case of curves (2) and (3), the concentrations of defects involved in one-step and two-step reactions are approximately equal. It is interesting to note that, irrespective of the way chosen, the modification of initial defects in different fibres results finally in approximately the same values of the induced refractive index at doses $\sim 5 - 6$ kJ cm^{-2} (Fig. 1).

4. Conclusions

The pre-exposure effect caused by a two-step photochemical reaction determines the dynamics of the refractive-index induction in all hydrogen-loaded fibres studied in the paper. A one-step photochemical reaction occurs simultaneously with the two-step reaction in all the fibres, the relation between intensities of these reactions being dependent on the fibre doping.

The two-step photochemical reaction mainly induces the refractive index in fibres having a comparatively weak

photosensitivity in the initial state, for example, in PSFs. These fibres are very convenient for studying the two-step photochemical reaction because the one-step reaction is weak in them and the one-step and two-step reactions are separated in their dose ranges.

The dynamics of refractive-index induction in fibres doped with antimony and germanium oxides and having a comparatively high photosensitivity in the initial state is mainly determined by the one-step reaction. In these fibres, the one-step and two-step photochemical reactions proceed in the same dose range, each of them contributing to the variation in the refractive index.

References

- [doi>](#) 1. Dyer P., Farley R., Giedl R., Byron K. *Electron. Lett.*, **30** (14), 1133 (1994).
2. Canning J., Pasman R., Sceats M.G. *Proc. Conf. Photosens. Quadr. Non-Linearity in Glass Waveguides* (Portland, Oregon, 1995) p.86.
3. Larionov Y.V., Rybaltovsky A.A., Semjonov S.L., et al., in *Bragg Gratings Photosensitivity and Poling in Glass Waveguides. Techn. Dig.* (Monterey, California, 2003) MC4.
4. Larionov Y.V., Rybaltovsky A.A., Semjonov S.L., et al. *Opt. Mater.* (in press).
- [doi>](#) 5. Canning J. *Optical Fiber Technology*, **6**, 275 (2000).
6. Dianov E., Neustruev V., in *Volokonno-opticheskie tekhnologii, materialy i ustroystva* (Fibreoptic Technologies, Materials, and Devices) (Moscow: Izd. N. Bochkareva, 1998).
- [doi>](#) 7. Larionov Yu.V., Rybaltovsky A.A., Semenov S.L., Kurzanov M.A., Obidin A.Z., Vartapetov S.K. *Kvantovaya Elektron.*, **33**, 919 (2003) [*Quantum Electron.*, **33**, 919 (2003)].
8. Dianov E.M. et al. *Tech. Dig. OFC'99* (San Diego, USA, 1999) PD25.
- [doi>](#) 9. Atezhev V.V., Vartapetov S.K., Zhukov A.N., Kurzanov M.A., Obidin A.Z. *Kvantovaya Elektron.*, **33**, 689 (2003) [*Quantum Electron.*, **33**, 689 (2003)].
- [doi>](#) 10. Ramecourt D., Niay P., Bernage P., Riant I., Douay M. *Electron. Lett.*, **35** (4), 329 (1999).
- [doi>](#) 11. Larionov Yu.V., Rybaltovsky A.A., Semenov S.L., Bubnov M.M., Dianov E.M. *Kvantovaya Elektron.*, **32**, 124 (2002) [*Quantum Electron.*, **32**, 124 (2002)].